# 2

# Distributed Models of Peritoneal Transport

Joanna Stachowska-Pietka and Jacek Waniewski
*Institute of Biocybernetics and Biomedical Engineering*
*Polish Academy of Sciences, Warsaw*
*Poland*

## 1. Introduction

There are several methods to model the process of water and solute transport during peritoneal dialysis (PD). The characteristics of the phenomena and the purpose of modelling influence the choice of methodology. Among others, the phenomenological models are commonly used in clinical and laboratory research. In peritoneal dialysis, the compartmental approach is widely used (membrane model, three-pore model). These kinds of models are based on phenomenological parameters, sometimes called "lumped parameters", because one parameter is used to describe the net result of several different processes that occur during dialysis. The main advantage of the compartmental approach is that it decreases substantially the number of parameters that have to be estimated, and therefore its application in clinical research is easier. However, in the compartmental approach, it is usually very difficult to connect the estimated parameters with the physiology and the local anatomy of the involved tissues. Therefore, these models have limited applications in the explanation of the changes that occur in the physiology of the peritoneal transport. For example, the membrane models describe exchange of fluid and solute between peritoneal cavity and plasma through the "peritoneal membrane". However, this approach does not take into account the anatomy and physiology of the peritoneal transport system and cannot be used for the explanation of the processes that occur in the tissue during the treatment.
Basic concepts and previous applications of distributed models are summarized in Section 2. A mathematical formulation of the distributed model for fluid and solute peritoneal transport is also presented in Section 2. The effective parameters, which characterize transport through the peritoneal transport system, PTS (i.e. the fluid and solute exchange between the peritoneal cavity and blood), can be estimated from the local physiological parameters of the distributed models. The comparisons between transport parameters applied in phenomenological description and those derived using a distributed approach, are presented in Sections 3 and 4 for fluid and solute transport, respectively. Typical distributed profiles of tissue hydration and solutes concentration in the tissue are presented in Section 5.

## 2. Distributed modelling of peritoneal transport

The first applications of the distributed model are dated to the early 1960s and were limited to the diffusive transport. Pipper et al. studied the exchange of gases between blood and artificial gas pockets within the body (Piiper, Canfield, and Rahn 1962). The transport of

gases between subcutaneous pockets and blood was studies in rats and piglets (Van Liew 1968; Collins 1981). The theory of heat and solute exchange between blood and tissue was investigated using distributed approach by Perl (Perl 1963, 1962). The first application of the distributed model for the description of the diffusive transport of small solutes was proposed by Patlak and Fenstermacher, in order to describe the transport from cerebrospinal fluid to the brain (Patlak and Fenstermacher 1975). The diffusive delivery of drugs to the human bladder during intravesical chemotherapy, as well as drug delivery from the skin surface to the dermis, has been also studied in normal and cancer tissue using distributed approach (Gupta, Wientjes, and Au 1995; Wientjes et al. 1993; Wientjes et al. 1991). The distributed model was also applied for the theoretical description of fluid and solute transport in solid tumors (Baxter and Jain 1989, 1990, 1991).

The need of the model that could relate the anatomy and local physiological processes with the observed outcome of the peritoneal transport was mentioned by Nolph, Miller, and Popovich (Nolph et al. 1980). One of the attempts in this direction was proposed by Dedrick, Flessner and colleagues. They considered a distributed approach, in which the spatial structure of the tissue with blood capillaries and lymphatics distributed at different distance from the peritoneal cavity, was taken into account (Dedrick et al. 1982; Flessner 2005; Flessner, Dedrick, and Schultz 1985). Another approach, based on the three-pore model, assumes existence of serial layers of two kinds: tissue and "peritoneal membrane" (Venturoli and Rippe 2001).

The application of distributed models in intraperitoneal therapies was initiated in the early eighties of the 20th century. Initially, the diffusive transport of gases between intraperitoneal pockets and blood was studied by Collins in 1981 (Collins 1981). In the peritoneal dialysis field the distributed approach was introduced by Dedrick, Flessner and colleagues (Dedrick et al. 1982; Flessner, Dedrick, and Schultz 1984). The distributed modelling of diffusive solute transport during peritoneal dialysis was also studied by Waniewski (Waniewski 2002). Further applications of the model in the peritoneal dialysis field were related to the transport of small, middle and macro -molecules in animal studies as well as in CAPD patients (Dedrick et al. 1982; Flessner 2001; Flessner, Dedrick, and Schultz 1985; Flessner et al. 1985; Flessner, Lofthouse, and Zakaria el 1997). The initial models of peritoneal solute transport considered interstitium as a rigid, porous medium with constant fluid void volume and intraperitoneal and interstitial hydrostatic pressures (Flessner, Dedrick, and Schultz 1984). This theoretical description was validated with experimental data from rats (Flessner, Dedrick, and Schultz 1985). In the later model of IgG peritoneal transport, the changes in interstitial and intraperitoneal pressure were taken into account according to experimental studies (Flessner 2001). The process of intraperitoneal drug delivery, especially for anticancer therapies, was also described using the distributed approach (Flessner 2001; Collins et al. 1982; Flessner 2009). The so far mentioned models were applied for diffusive and convective solute transport. Seames, Moncrief and Popovich were the first who investigated osmotically driven fluid and solute transport during peritoneal dwell (Seames, Moncrief, and Popovich 1990). However, their attempt was later disproved by animal experiments (Flessner et al. 2003; Flessner 1994). Further investigations by Leypoldt and Henderson were focused on solute transport driven by diffusion and ultrafiltration from blood and interactions of the solute with the tissue (Leypoldt 1993; Leypoldt and Henderson 1992). A new attempt to apply a distributed approach to model impact of chronic peritoneal inflammation from sterile solutions and structural changes within the tissue on the solute and water transport was undertaken recently by Flessner et al. (Flessner et al. 2006).

The distributed model of fluid absorption was proposed by Stachowska-Pietka et al. and applied for the analysis changes in the tissue caused by infusion of isotonic solution into the peritoneal cavity (Stachowska-Pietka et al. 2005; Stachowska-Pietka et al. 2006). This model can be applied to describe situation at the end of a dwell with hypertonic solution, when the osmotic pressure decreases and the intraperitoneal hydrostatic pressure is the main transport force. The osmotically driven glucose transport was modelled by Cherniha, Waniewski and co-authors (Cherniha and Waniewski 2005; Waniewski et al. 2007; Waniewski, Stachowska-Pietka, and Flessner 2009). These authors where able to predict high ultrafiltration from blood to the peritoneal cavity and positive interstitial pressure profiles assuming a high value of reflection coefficient for glucose in the capillary wall and a low value of reflection coefficient for glucose in the tissue. Further extensions of this model were suggested (Stachowska-Pietka, Waniewski, and Lindholm 2010; Stachowska-Pietka 2010; Stachowska-Pietka and Waniewski 2011). In this new approach, the variability of dialysis fluid volume, hydrostatic pressure and solute concentrations with dwell time were additionally taken into account and yielded a good agreement of the theoretical description and clinical data. A distributed model that takes into account also the two phase structure of the tissue and allows for the modelling of bidirectional fluid and macromolecular transport during PD was recently formulated (Stachowska-Pietka, Waniewski, and Lindholm 2010; Stachowska-Pietka 2010).

### 2.1 Basic concepts

The distributed approach takes into account the spatial distribution of the peritoneal transport system (PTS) components. Typically, this concept includes the microcirculatory exchange vessels that are assumed to be uniformly distributed within the tissue. However, this simplifying assumption can in general be omitted and the variability of the tissue space and structure can be taken into account. In order to describe the distributed structure of PTS, the methods of partial differential equation (instead of ordinary differential equations) should be applied. As a result, the changes in the spatial distribution of solutes and fluid in the tissue with time can be modelled.

Peritoneal fluid and solute exchange concerns all the organs that surround peritoneal cavity. It is assumed that tissue is perfused with blood by capillaries, which are placed at different distance from the peritoneal surface (Figure 1).

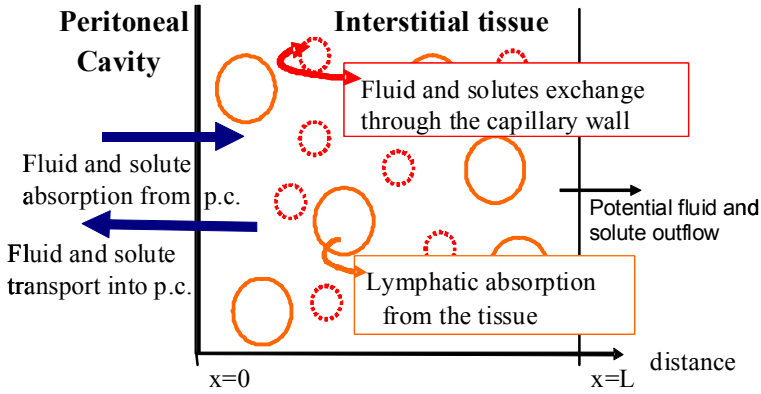


Fig. 1. Fluid and solute transport pathways during peritoneal dialysis: dashed, red circles – blood capillaries walls, solid, orange circles – lymphatic capillaries

Lymphatic absorption plays an important role in the process of regulation of fluid and solute transport within the tissue. The tissue properties, including the spatial distribution of blood and lymph capillaries, are idealized in the distributed modelling by the assumption that blood and lymph capillaries are uniformly distributed within the tissue and that the interstitium is a deformable, porous medium, see Figure 1 (Flessner 2001; Waniewski 2001). The difference in solute concentration between blood and dialysis fluid results in a quasi-continuous spatially variable concentration profile. Moreover, fluid infusion into the peritoneal cavity induces increase of interstitial hydrostatic pressure and results in fluid transport within the tissue. The tissue hydrostatic pressure equilibrates with the intraperitoneal hydrostatic pressure at the peritoneal surface, and decreases with the distance from the peritoneal cavity.

### 2.1.1 Structure of the peritoneal transport systems and its barriers

Once water and solutes leave the peritoneal cavity and enter the adjacent tissue they penetrate to its deeper parts, c.f. Figure 1. In the tissue, fluid and solute partly cross the heteroporous capillary wall and are washed out by the blood stream, whereas another part is absorbed from the tissue by local lymphatics. A part of the fluid and solute accumulates in the tissue. In some situations, fluid and solutes can leave the tissue on its other side, as in the case of the intestinal wall or in some experiments with the impermeable outer surface (skin) removed (Flessner 1994). Figure 1 summarizes the fluid and solute transport pathways.

Two main transport barriers for peritoneal fluid and solute transport are considered in the distributed approach. On the basis of experimental data it was found that: 1) the heteroporous structure of the capillary wall, and 2) interstitium, are significant barriers of the peritoneal transport system (Flessner 2005). The experimental studies showed that interstitium is the most important barrier for the transport of fluid and selected solutes across the tissue. In contrast, some authors considered also the mesothelium as a substantial transport barrier and modeled it as a semipermeable membrane with the properties analogous to the that of the endothelium (Seames, Moncrief, and Popovich 1990). They analyzed the transport of water, BUN, creatinine, glucose and inulin. They fitted the model to the data on intraperitoneal volume and solute concentrations in dialysate and blood and predicted negative values of interstitial hydrostatic pressure (Seames, Moncrief, and Popovich 1990). However, later studies disproved this assumption and found the positive interstitial pressure profiles in the tissue (Flessner et al. 2003).

### 2.1.2 Fluid and solute void volume

The fluid space within the interstitium can be described using the interstitial fluid void volume ratio, $\theta$, that is defined as the fraction of the interstitial space that is available for interstitial fluid (non-dimensional, being the ratio of volume over volume). Typically, at physiological equilibrium, this value remains around 15% - 18%, and may be doubled during peritoneal dialysis (Zakaria, Lofthouse, and Flessner 2000, 1999). The fraction of solute interstitial void volume, $\theta_S$, i.e., the fraction of tissue volume effectively available to the solute $S$, depends on the solute molecular size, and in the case of large macromolecules can be significantly smaller than that for fluid. Experimental studies showed that distribution of the solute macromolecules can be restricted to even 50% of $\theta$ (Wiig et al. 1992). Therefore, in general $\theta_S \le \theta$.

The interstitial fluid void volume ratio as a function of interstitial hydrostatic pressure derived on the basis of experimental studies is presented in Figure 2, c.f. (Cherniha and Waniewski 2005; Stachowska-Pietka et al. 2005; Stachowska-Pietka et al. 2006).

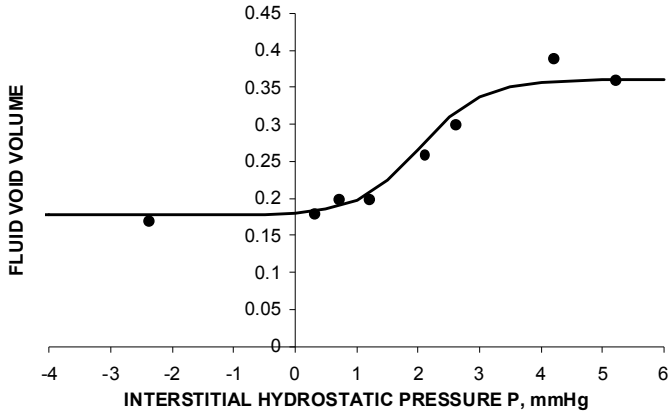


Fig. 2. The experimental data of interstitial fluid void volume ratio measured in the rat skeletal muscle and signed by solid circles (Zakaria, Lofthouse, and Flessner 1999) and the fitted interstitial fluid void volume ratio curve, $\theta$, as a function of interstitial pressure, $P$.

This approach reflects the experimental findings showing that interstitial fluid void volume ratio may increase initially rapidly (for positive, low values of interstitial pressure), whereas there is no effect of further increasing of $P$ if $\theta$ reaches its maximal value, $\theta_{MAX}$. The interstitial fluid void volume, $\theta$, can be mathematically described as (Stachowska-Pietka et al. 2006):

$$\theta = \theta_{MIN} + \frac{\theta_{MAX} - \theta_{MIN}}{1 + \left( \frac{\theta_{MAX} - \theta_{MIN}}{\theta_0 - \theta_{MIN}} - 1 \right) e^{-\beta (P - P_0)}} \tag{1}$$

where $\theta_{MIN} = 0.177$ and $\theta_{MAX} = 0.36$ are respectively minimal and maximal values of the fluid void volume, $\theta_0 = 0.18$ is the fluid void volume for $P = P_0 = 0$ mmHg, $\beta = 2.019$ mmHg$^{-1}$, and $P_0$ is the initial value of interstitial hydrostatic pressure measured in mmHg, see Figure 2. A particular case of this general formula was considered previously by An and Salathe (An and Salathe 1976). They were the first, who proposed the explicit formula for the fluid void volume as a function of interstitial pressure, assuming erroneously that $\theta_{MIN} = 0$ and $\theta_{MAX} = 1$.

### 2.2 Distributed model of fluid transport

The changes in the total tissue volume are considered to be small enough to assume the constant total tissue volume. Therefore, the whole tissue is considered as not expendable, whereas the interstitial compliance and changes in the tissue hydration are taken into account. Under this condition, the equation for the changes in the fraction of the interstitial fluid void volume ratio can be described using the volume balance of the interstitium as follows (Stachowska-Pietka et al. 2006; Stachowska-Pietka et al. 2005; Flessner 2001):

$$\frac{\partial \theta}{\partial t} = -\frac{\partial j_V}{\partial x} + q_V \tag{2}$$

where $\theta$ is the fraction of the interstitial fluid volume over the total tissue volume, further on called as the void volume, $j_V$ is the volumetric fluid flux across the interstitium, $q_V$ is the rate of the net fluid flow into the tissue from the internal sources (sinks) such as blood or lymphatic capillaries per unit tissue volume, $t$ is the dwell time, and $x$ is the distance measured from the peritoneal cavity. Note, that volumetric flux, $j_V$, is defined as volumetric flow (in ml/min) per unit surface (in cm²) perpendicular to its direction, i.e., the unit of flux is cm/min. The unit of local volumetric flow density, $q_V$, is 1/min, i.e., as for volumetric flow (in ml/min) per unit volume (in mL). The orientations of specific fluid fluxes are presented in Figure 3.

Fluid flux across the interstitium depends on the local tissue hydraulic conductivity, $K$, and local interstitial hydrostatic pressure gradient, $\partial P / \partial x$. Moreover, the osmotic agent (crystalloid or colloid) may exert osmotic effect on the fluid. These effects can be taken into account by including the role of local tissue osmotic gradients into the model. In particular, the impact of the oncotic gradient exerted by proteins was previously included in the Darcy formula by Taylor et al. (Taylor, Bert, and Bowen 1990). Thus, the volumetric fluid flux across the interstitium may be calculated by the extended Darcy law as follows (Waniewski, Stachowska-Pietka, and Flessner 2009; Waniewski et al. 2007):

$$j_V = -K\left(\frac{\partial P}{\partial x} - \sum_{S=1,\ldots,N} {\sigma_S}^T \cdot RT \cdot \frac{\partial C_S}{\partial x}\right) \tag{3}$$

where ${\sigma_S}^T$ is the reflection coefficient (positive for osmotically active solutes in the tissue), $C_S$ is the concentration of solute in the tissue, and solutes are indexed by $S$ from 1 to $N$.

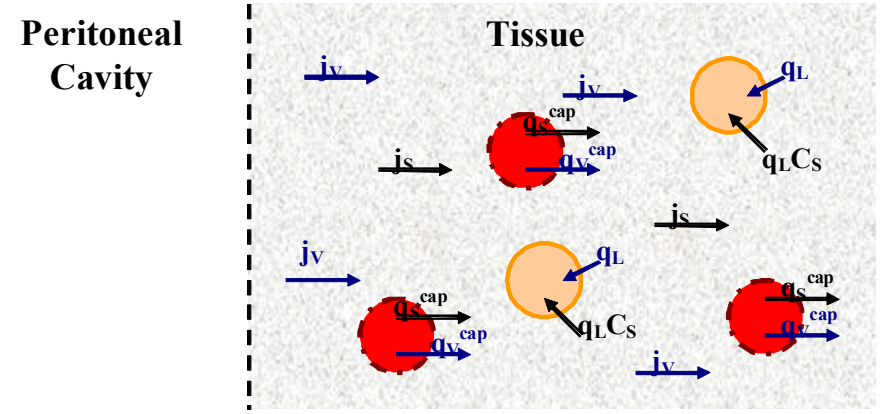


Fig. 3. Scheme of fluid and solute transport and positive orientations of each flux as modelled by the distributed approach: dashed circles – blood capillaries walls, solid circles – lymphatic capillaries.

Fluid flow between tissue and circulatory system, ${q_V}^{cap}$, can occur through the capillary wall in both directions: into and from the tissue. In addition, the final net inflow of fluid to the tissue is typically smaller due to the local tissue lymphatic absorption. Therefore, the net fluid inflow into the tissue is given as:

$$q_V = q_V^{cap} - q_L \tag{4}$$

where $q_V^{cap}$ is the net fluid flow through the capillary wall into the tissue, and $q_L$ is the rate of lymphatic absorption in the tissue. For the calculation of the fluid flow across capillary wall, the three-pore model or the membrane model can be applied. According to both approaches, the fluid flow across the capillary wall, $q_V^{cap}$, is driven by the hydrostatic (first term) and osmotic pressure (second term) differences that are exerted through the capillary wall. In particular, if the membrane model is applied for the microvascular exchange of fluid, net fluid flow across the capillary wall to the tissue can be calculated as (Stachowska-Pietka et al. 2006; Waniewski, Stachowska-Pietka, and Flessner 2009):

$$q_V^{cap} = L_P a\left(P_B - P\right) - L_P a \sum_{S=1,\ldots,N} \sigma_S^{cap} \cdot RT \cdot \left(C_{B,S} - C_S\right) \tag{5}$$

where $P_B$ and $C_{B,S}$ are the hydrostatic pressure and solute concentration in the blood, respectively, $P$ and $C_S$ are interstitial hydrostatic pressure and solute concentration in the tissue, respectively, $L_P a$ and $\sigma_S^{cap}$ are the capillary wall hydraulic conductance and reflection coefficient of the capillary wall, respectively. If the three-pore model for the microvascular exchange across capillary wall is applied, the fluid transport through each type of pore should be calculated separately, and summed up.

Equation (1) specifies the interstitial fluid void volume, $\theta$, as a function of interstitial pressure, $P$. Therefore, the rate of change of $\theta$ can be transformed as $\frac{\partial \theta}{\partial t} = \frac{d\theta}{dP} \cdot \frac{\partial P}{\partial t}$ and equation (2) for time evolution of variable $\theta$ can be converted to the following equation for the time evolution of variable $P$ (Stachowska-Pietka et al. 2006):

$$\frac{d\theta}{dP} \cdot \frac{\partial P}{\partial t} = -\frac{\partial}{\partial x} j_V + q_V \tag{6}$$

In order to find theoretical solution, these equations must be combined with equations for the transport of solutes. In general, the transport parameters in equations (2) - (5), such as $K$, $q_L$, $L_P a$, $\sigma_S^T$, $\sigma_S^{cap}$ can be assumed constant for some approximate considerations (Waniewski 2001; Flessner 2001). However, physiological data suggest that in more realistic modelling, the relationship between the parameters and the tissue properties should be taken into account. In particular, the dependence of tissue hydration, hydraulic conductivity, or lymphatic absorption on the interstitial hydrostatic pressure as well as the vasodilation induced by hyperosmotic dialysis fluid should be considered. Therefore, in numerical simulations of distributed models, some of the transport parameters (such as $K$, $q_L$, $L_P a$) are typically functions of model variables (solute concentration in the tissue, $C_S$, interstitial hydrostatic pressure, $P$, and also indirectly of interstitial fluid void volume ratio, $\theta$) and dwell time, $t$. The specific forms of these functions can be found elsewhere (Stachowska-Pietka et al. 2006; Waniewski, Stachowska-Pietka, and Flessner 2009; Stachowska-Pietka 2010). Initial and boundary conditions for this problem are well define and were previously discussed in details (Stachowska-Pietka et al. 2006; Stachowska-Pietka 2010; Stachowska-Pietka et al. 2005).

### 2.3 Distributed model of solute transport

The solute concentration profiles within the tissue can be derived from the equation on the local solute mass balance using a partial differential equation for local solute balance as (Stachowska-Pietka et al. 2007; Waniewski 2002; Waniewski, Stachowska-Pietka, and Flessner 2009; Flessner 2001):

$$\frac{\partial(\theta_S \cdot C_S)}{\partial t} = -\frac{\partial j_S}{\partial x} + q_S \tag{7}$$

where $\theta_S$ is the fraction of interstitial fluid void volume ratio, $\theta$, available for the distribution of solute $S$, $C_S$ is the solute concentration in the interstitial fluid, $j_S$ is the solute flux across the tissue, $q_S$ is the rate of the net solute inflow to the tissue from the external sources/sinks, such as blood or lymph, $x$ is the distance measured from the peritoneal surface, and $t$ is time. The solute flux across the tissue, $j_S$, is defined as the solute flow (in mmol/min) per unit surface (in cm$^2$) perpendicular to its direction, i.e., the unit of flux is mmol/min/cm$^2$. The unit of local solute flow density, $q_S$, is mmol/min/mL, i.e., as for solute flow (in mmol/min) per unit volume (in mL). The orientations of solute fluxes are presented in Figure 3.

Solute flux across the tissue comprises two components. The diffusive transport of solute depends on the local concentration gradient, whereas fluid flux across the tissue induces its convective transport. Therefore, the solute flux across the tissue can be calculated as follows (Stachowska-Pietka et al. 2007; Waniewski 2002; Waniewski, Stachowska-Pietka, and Flessner 2009; Flessner 2001):

$$j_S = -D_S{}^T \frac{\partial C_S}{\partial x} + s_S{}^T \cdot j_V \cdot C_S \tag{8}$$

where $D_S{}^T$ is the diffusivity of solute $S$ in the tissue, $s_S{}^T$ is sieving coefficient of solute in the tissue, and $j_V$ is the volumetric fluid flux across the tissue. Note, that for homogenous structure $\sigma_S{}^T = 1 - s_S{}^T$ is the tissue reflection coefficient of solute $S$.

The net changes in the solute amount in the tissue are considered to be caused by the local microvascular exchange between blood and tissue through the capillary wall, decreased by the solute absorption from the tissue by local lymphatics:

$$q_S = q_S{}^{cap} - q_L \cdot C_S \tag{9}$$

where $q_S{}^{cap}$ in the net solute flux across the capillary wall into the tissue, and $q_L$ is the rate of local lymphatic absorption. Depending on the purpose of the study, the solute transport between blood and tissue can be calculated according to the three-pore model or the membrane model. In general, solute flux across the capillary wall is driven by the solute concentration difference between blood and tissue, $C_{B,S} - C_S$, and by the convective fluid flow across the capillary wall, $q_V{}^{cap}$. In particular, if the membrane model is applied for the microvascular exchange, the solute net flux across the capillary wall to the tissue can be calculated as (Waniewski et al. 2007; Waniewski, Stachowska-Pietka, and Flessner 2009):

$$q_S{}^{cap} = p_S a\left(C_{B,S} - C_S\right) + s_S{}^{cap} \cdot q_V{}^{cap} \cdot \left[ f C_{B,S} + (1-f) \cdot C_S \right] \tag{10}$$

where $p_S a$ is the diffusive permeability of solute $S$ through the capillary wall, $s_S{}^{cap}$ is sieving coefficient for solute in the capillary wall, and $f$ is the weighting factor within the range from 0 to 1, which in general can be calculated from the fluid flow across the capillary wall according to the formula for Peclet number. Note, that $\sigma_S{}^{cap} = 1 - s_S{}^{cap}$ is the capillary wall reflection coefficient for solute $S$. In the case of a three-pore model for the microvascular exchange across the capillary wall it can be described as the sum of solute fluxes through each type of the pore.

Equation (7) together with equations (8) - (10) for $j_S$ and $q_S$ may be analyzed theoretically for constant values of $\theta_S$, constant transport parameters such as $D_S{}^T$, $s_S{}^T$, $p_S a$, $s_S{}^{cap}$, and for given fluid transport characteristics $j_V$ and $q_V{}^{cap}$. However, in the general case, equation (7) must be coupled with equation (6) for time evolution of $P$, in order to calculate $\theta$ and then $\theta_S$. Furthermore, the dynamic changes in the transport parameters, caused by the changes in tissue hydration and vasodilation of the capillary bed, make $D_S{}^T$ and $p_S a$ functions of $P$ (or $\theta$), $C_S$ and dwell time, $t$. The specific forms of these functions can be found elsewhere (Stachowska-Pietka 2010; Stachowska-Pietka et al. 2006; Waniewski, Stachowska-Pietka, and Flessner 2009). The details concerning initial and boundary conditions for solute and fluid peritoneal transport can be found elsewhere (Stachowska-Pietka and Waniewski 2011; Stachowska-Pietka 2010; Waniewski, Stachowska-Pietka, and Flessner 2009, Waniewski 2001, 2002).

## 3. Modelling of fluid transport

The purpose of this section is to present relationships between the net fluid transport parameters for the transport between blood and dialysis fluid in the peritoneal cavity (as estimated using phenomenological models of peritoneal dialysis in clinical and experimental studies), and the separate characteristics of the capillary wall and interstitial transport barriers as well as the distributed geometry of peritoneal transport system (PTS). Two simplified versions of the distributed model for fluid peritoneal transport are analysed assuming steady state conditions. The effective permeability of the tissue is analysed for the simplified model in which fluid transport is driven by hydrostatic pressure difference, causing fluid absorption. In order to present osmotic properties of PTS, the distributed model of osmotic fluid flow is presented, in which water absorption from the peritoneal cavity is neglected.

In order to evaluate effective transport parameters from the distributed model, which can be compare with the experimental values, one should refer to the net fluid flow instead of fluid flux. In general, the net fluid flow can be calculated from the fluid flux by multiplying by the effective peritoneal surface area $A$ in cm². Therefore $J_V = A \cdot j_V$ is the fluid flow described in mL/min, and $A \approx 6000$ cm². More details concerning results presented in this section can be found in (Waniewski, Stachowska-Pietka, and Flessner 2009).

### 3.1 Effective hydraulic conductivity

A simple version of the distributed model with fluid flow induced only by hydrostatic pressure may be applied for the derivation of the description of the flux across the tissue peritoneal surface, $j_V\left(t_{steady}, x = 0\right) = j_V{}^{perit}$, and the effective hydraulic conductivity for fluid

at time $t_{steady}$, when the system reaches its steady-state. Therefore, equation (3) for fluid transport across tissue can be simplified to the from $j_V = -K\frac{\partial P}{\partial x}$, whereas fluid transport across capillary wall is given by $q_V{}^{cap} = L_P a\left(P_B - P\right)$. In this case, the fluid flow across the peritoneal surface (i.e. fluid flux multiplied by effective peritoneal surface area) depends on the hydrostatic pressure difference between peritoneal cavity and the tissue and can be described by the following formula (Waniewski, Stachowska-Pietka, and Flessner 2009):

$$J_V{}^{perit} = memL_P a\left(P_D - P^{eq}\right) \tag{11}$$

where $P_D$ and $P^{eq}$ are hydrostatic pressures in the peritoneal cavity and tissue, respectively, and $memL_P a$ is the effective hydraulic conductivity for transport between blood and dialysate that is calculated as:

$$memL_P a = A \cdot \tanh(\varphi)\sqrt{K \cdot L_P a} \tag{12}$$

with $\varphi = L / \Lambda_F$, L - tissue width, and $\Lambda_F = \sqrt{K / L_P a}$ - fluid penetration depth in the tissue, $K$ - tissue hydraulic conductivity, $L_P a$ - hydraulic conductance of capillary wall, $A$ - effective peritoneal surface area. Furthermore, assuming that tissue width is much higher than the fluid penetration depth, $\Lambda_F << L$, i.e. $\varphi >> 1$, one can get the following, simplified formula for the effective hydraulic conductivity for transport between blood and dialysate:

$$memL_P a = A\sqrt{K \cdot L_P a} \tag{13}$$

Some exemplary values of fluid penetration depth, effective hydraulic conductivity of PTS and the corresponding values of tissue and capillary wall transport are presented in Table 1.

*Remark* 1. Formula (13) can be transformed to $memL_P a = A \cdot L_P a \cdot \Lambda_F$, which means that the fluid transport may be considered, according to the distributed model, as proceeding directly between blood and dialysis fluid across the total capillary wall surface within the tissue layer of the width $\Lambda_F$ with hydraulic conductance $L_p a$, as this capillary would be immersed directly in dialysis fluid (Waniewski, Stachowska-Pietka, and Flessner 2009).

*Remark* 2. Formula (13) can be alternatively transformed to $memL_P a = A \cdot K / \Lambda_F$ indicating that the same fluid transport may be considered also as proceeding between blood and dialysis fluid across the tissue layer with hydraulic conductivity $K$ and width $\Lambda_F$ (which is fluid penetration depth) without any interference from blood flow in the capillaries; however, $\Lambda_F$ depends on $L_p a$ (Waniewski, Stachowska-Pietka, and Flessner 2009).

*Remark* 3. The maximal possible value of $memL_P a$ is $A \cdot L_P a \cdot L$, which would happen if the fluid penetrated fully the whole tissue layer, and in this case the effective hydraulic conductivity of distributed system would be equal to the total hydraulic conductance for the whole capillary bed in the tissue (Waniewski, Stachowska-Pietka, and Flessner 2009).

| Parameter | Range of values |
|---|---|
| Assumed/adjusted: | |
| $K\,10^4$ , $cm^2 min^{-1} mmHg^{-1}$ | 0.139 |
| $L_P a\,10^4$ , $ml \cdot min^{-1} mmHg^{-1} g^{-1}$ | 1.48 – 3.66 |
| Derived: | |
| $\Lambda_F$ , cm | 0.19 – 0.31 |
| $memL_P a$ , $ml \cdot min^{-1} mmHg^{-1}$ | 0.27 – 0.43 |

Table 1. Theoretical values of transport parameters assumed in computer simulations and the corresponding values of effective transport parameters of PTS estimated for A = 6000 $cm^2$: $K$ – tissue hydraulic conductivity, $L_P a$ - capillary wall hydraulic conductance, A – effective peritoneal surface area, $\Lambda_F$ - fluid penetration depth, $memL_P a$ - effective hydraulic conductivity of PTS (Waniewski, Stachowska-Pietka, and Flessner 2009).

### 3.2 Effective reflection coefficient and osmotic conductance

In this section a model with a single osmotic agent that induces osmotic fluid flow between blood and the peritoneal cavity is discussed. The hydrostatic pressure gradient in the tissue also contributes to the fluid flow, but the hydrostatic pressure difference across the capillary wall is neglected by assuming, for example, that it is approximately balanced by oncotic pressure difference. This approximation may be used only for the description of osmotic ultrafiltration induced by a high concentration of a crystalloid osmotic agent. Therefore, in the case of a single osmotic agent (as glucose), equation (3) for fluid flux across the tissue is $j_V = -K\left(\frac{\partial P}{\partial x} - \sigma^T \frac{\partial C}{\partial x}\right)$, and equation (5) is $q_V{}^{cap} = L_P a \cdot \sigma^{cap} RT\left(C_B - C\right)$. Note, that for the sake of simplicity, in the case of single solute, the bottom index S for solute can be omitted. If the solute (e.g., glucose) concentration profile in the tissue may be approximately described by the exponential function with the solute penetration depth $\Lambda$, i.e. as $C = C_B + \left(C_D - C_B\right)\exp\left(-x/\Lambda\right)$, the steady state fluid flow across the peritoneal surface can approximated by the following formula (Waniewski, Stachowska-Pietka, and Flessner 2009):

$$J_V{}^{perit} = -memL_P a \cdot \sigma^{eff} \cdot RT\left(C_D - C^{eq}\right) \tag{14}$$

where $memL_P a$ is the effective hydraulic conductivity of the peritoneal transport system, $C_D$ and $C^{eq}$ are solute concentrations in dialysate and tissue, respectively, and $\sigma^{eff}$ is the effective reflection coefficient for solute transport between peritoneal cavity and blood given by (Waniewski, Stachowska-Pietka, and Flessner 2009):

$$\sigma^{eff} = \frac{\sigma^{cap}}{\alpha}\left(1 - e^{-L/\Lambda}\right) \tag{15}$$

where $\alpha = \Lambda_F / \Lambda$ is the ratio of fluid to solute penetration depth, $\sigma^{cap}$ is the capillary wall reflection coefficient to solute S. Moreover, assuming that the tissue width is much higher than the solute penetration depth, i.e. $L >> \Lambda$ , one can get the following simplified formula for the effective reflection coefficient of PTS (Waniewski, Stachowska-Pietka, and Flessner 2009):

$$\sigma^{eff} = \frac{\sigma^{cap}}{\alpha} \tag{16}$$

*Remark* 1. The value of the effective reflection coefficient for particular solute transport between peritoneal cavity and blood, $\sigma^{eff}$, can not exceed the value of the capillary wall reflection coefficient for this solute, $\sigma^{cap}$, i.e. $\sigma^{eff} \le \sigma^{cap}$.
*Remark* 2. The effective reflection coefficient can be calculated from the capillary wall reflection coefficient, after dividing by the ratio of fluid to solute penetration depth. Moreover, if necessary, this value should be additionally decreased by the formula $\left(1 - e^{-L/\Lambda}\right)$. As the result, the distributed geometry of the capillary bed yields a substantial decrease in the effective reflection coefficient for crystalloid osmotic agents compared with their reflection coefficient in the capillary wall. Numerical simulations suggest 7-20 times lower values of $\sigma^{eff}$ if compared to $\sigma^{cap}$ (see, Table 2 and (Waniewski, Stachowska-Pietka, and Flessner 2009)).
*Remark* 3. The effective reflection coefficient for the transport between peritoneal cavity and blood depends not only on the sieving properties of the capillary wall, but is also related to the tissue transport properties, since both fluid and solute penetration depths depends on the local tissue and capillary wall permeabilities.
*Remark* 4. The effective osmotic conductance for the transport between peritoneal cavity and blood depends on both tissue and capillary wall transport characteristics and can be calculated as the effective hydraulic conductivity described by equation (13), multiplied by the effective reflection coefficient, described by equation (15), c.f. equation (14) (Waniewski, Stachowska-Pietka, and Flessner 2009):

$$memOsmCond = \sigma^{eff} memL_p a \tag{17}$$

In Table 2, some typical values of effective reflection coefficient and osmotic conductance of PTS are derived for glucose in the case of clinical dialysis.

| Parameter | Range of values |
|---|---|
| Assumed/adjusted: | |
| $\sigma^{cap}$ | 0.16 – 0.46 |
| Derived: | |
| $\Lambda$, cm | 0.015 – 0.017 |
| $\alpha$ | 11.40 – 20.86 |
| $\sigma^{eff}$ | 0.014 – 0.022 |
| *memOsmCond*, (ml/min)/(mmol/l) | 0.116 |

Table 2. Theoretical values of glucose transport parameters assumed in computer simulations and the corresponding values of effective transport parameters of PTS (Waniewski, Stachowska-Pietka, and Flessner 2009): $\sigma^{cap}$ - capillary wall reflection coefficient, $\Lambda$ - solute penetration depth, $\alpha$ - ratio of fluid to solute penetration depth, $\sigma^{eff}$ - effective reflection coefficient of PTS, *memOsmCond* – effective osmotic conductance of PTS.

## 4. Modelling of solute transport

During peritoneal dialysis solutes, such as osmotic agents, buffer solutes, additives and drugs, are transported from dialysis fluid to the tissue, and inside the tissue are absorbed to

blood and lymph. On the other hand, solutes, which are to be removed with peritoneal dialysis, are transported first from blood to the tissue and there they are partly absorbed with lymph and partly transported to dialysis fluid. The contribution of blood and lymph flows to the solute gradient, created within the tissue due to the presence of dialysis fluid at the tissue surface, results in characteristic solute concentration profiles within the tissue. For some solutes, diffusive transport prevails (as for small molecules), but the role of convective transport through the capillary wall and (convective) absorption with lymph increases with the increased molecular weight. In particular, in the case of macromolecules, both types of convective transport should be considered.

Therefore, for small molecules such as urea, creatinine, the simplified version of the distributed model with pure diffusive transport can be considered. In this case, simple relationships between net solute transport characteristics such as effective diffusivity across PTS, solute penetration depth and effective blood flow, and corresponding local distributed parameters are presented. The impact of combined diffusive and convective transport on derived effective characteristics is analysed in Section 4.2. In particular, the comparison between diffusive and convective penetration depth, as well as the analysis of effective sieving coefficient for macromolecules is analysed.

Note, that all results presented in this section were derived for the steady state conditions. Moreover, to compare the effective solute transport parameters with the experimental one, the solute flux from the peritoneal cavity is multiplied by the effective peritoneal surface area, A. This transforms the equation for solute flux, $j_S$, into the equation for solute flow, $J_S = A \cdot j_S$, expressed in mmol/min. More details concerning models and the derivation of the expressions for effective transport parameters can be found in (Waniewski 2002, 2001). The bottom index *S*, which denotes solute, was omitted in this section for the sake of simplicity.

### 4.1 Diffusive solute transport between blood and the peritoneal cavity

In this section the relationships between the net diffusive mass transport coefficients for the solute transport between blood and dialysis fluid and the local physiology based transport parameters of distributed models are analyzed. Moreover, the formulas for the solute diffusive penetration depth and effective peritoneal blood flow are derived. Therefore, a simplified model of pure diffusive transport across the tissue is analysed at the steady state with the solute flux across the tissue given by $j_S = -D^T \frac{\partial C}{\partial x}$ and solute transport across capillary wall described by equation (10). Note, that equation (10) can be grouped in the following way: $q_S{}^{cap} = k^{cap} C_B - k^T C$, where $k^{cap} = p_S a + s^{cap} q_V{}^{cap} f$ is a unidirectional clearance for transport between blood and tissue, and $k^T = p_S a + s^{cap} q_V{}^{cap} (1 - f)$ is a unidirectional clearance for transport from tissue to blood (Waniewski 2002).

#### 4.1.1 Effective diffusive mass transport parameter

At the steady state, the solute flow from the peritoneal cavity to the tissue can be presented in analogy to the membrane models in the following way (Waniewski 2002):

$$J_S{}^{perit} = memKBD_S \left( C_D - \kappa C_B \right) \tag{18}$$

where $C_D$ and $C_B$ are solute concentrations in dialysate and blood, respectively, $memKBD_S$ is the effective diffusive mass transport parameter for solute $S$, and $\kappa$ describes the ratio of the equilibrium concentration of solute in the tissue over its concentration in blood and can be calculated as $\kappa = k^{cap} / \left(k^T + q_L\right)$. In this case, the effective diffusive mass transport parameter for solute $S$ can be approximated from the formula (Waniewski 2002, 2001):

$$memKBD_S = A\sqrt{D^T \left(k^T + q_L\right)} \tag{19}$$

Theoretical values of effective diffusive mass transport parameter derived from the distributed model compared with the experimental values are presented in Figure 4 and in Tables 3 and 4.

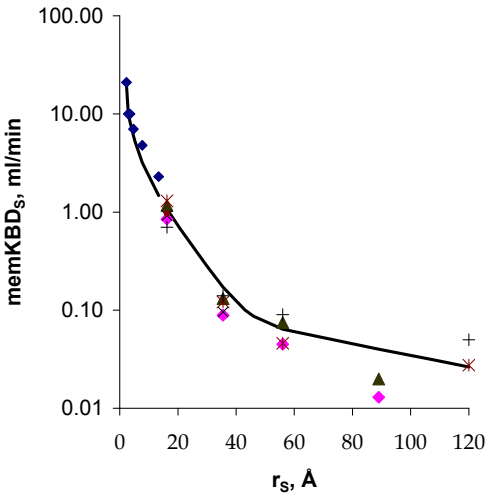


Fig. 4. Theoretical values of effective diffusive mass transport parameter derived from the distributed model (solid line, assuming A=1 m²) and the experimental values: * (Rippe and Stelin 1989), + (Kagan et al. 1990),▲ (Imholz et al. 1993), ♦ (Pannekeet et al. 1995), after (Waniewski 2001).

*Remark* 1. If one neglects convective transport across the capillary wall and the tissue lymphatic absorption, the effective diffusive mass transport parameter for solute $S$ can be calculated from a simplified formula (Dedrick et al. 1982):

$$memKBD_S = A\sqrt{D^T \cdot p_S a} \tag{20}$$

*Remark* 2. The important difference between equations (18) and the corresponding equation for diffusive solute transport according to the phenomenological membrane approach is the presence of coefficient $\kappa$ in equation (18). Therefore, according to the distributed model (equation (18)), the equilibration level for a solute in dialysate is not its concentration in blood, $C_B$, as it is in the membrane model, but its equilibrium concentration in the tissue $C^{eq} = \kappa C_B$. In typical physiological conditions of the transport through the capillary wall, $\kappa$

is close to 1 for small and middle molecules, but substantially lower than 1 for macromolecules (Waniewski 2002, 2001). Therefore, the correction for $\kappa$ is practically important only for macromolecules. In this case, the membrane model may underestimate the effective diffusive mass transport parameter. In fact, the equilibrium level for total protein five times lower than blood concentration was observed in experiments in dogs with prolonged accumulation of the lost protein in dialysate (Rubin et al. 1985). The typical values of $\kappa$ for proteins are presented in Table 3.

| Solute | MW | $\Lambda_{Dif}$, mm | $\kappa$ | $memKBD_S$, ml/min |
|---|---|---|---|---|
| $\beta_2$-microglobulin | 11 800 | 0.385 | 0.986 | 1.091 |
| myoglobin | 17 000 | 0.465 | 0.961 | 0.704 |
| α-globulin | 45 000 | 0.652 | 0.811 | 0.348 |
| albumin | 68 000 | 0.731 | 0.656 | 0.262 |
| transferin | 90 000 | 0.746 | 0.475 | 0.212 |
| haptoglobin | 100 000 | 0.732 | 0.430 | 0.202 |
| IgG | 150 000 | 0.667 | 0.351 | 0.182 |
| $\alpha_2$-macroglobin | 820 000 | 0.529 | 0.277 | 0.144 |
| IgM | 900 000 | 0.456 | 0.212 | 0.124 |

Table 3. Solute diffusive penetration depth, $\Lambda_{Dif}$, the ratio of the equilibrium concentration of solute in the tissue over its concentration in blood, $\kappa$, and effective diffusive transport parameter, $memKBD_S$, estimated from the distributed model assuming $A$=1 m² (Waniewski 2002).

#### 4.1.2 Diffusive solute penetration depth

The solute concentration distribution within the tissue (assuming only diffusive transport across the tissue) is described in the steady state by the following equation:

$$\frac{\partial^2 C}{\partial x^2} = \left(C^{eq} - \kappa C_B\right) / \Lambda_{Dif}^2 \tag{21}$$

where $C^{eq}$ is the solute concentration in the tissue at equilibrium, and $\Lambda_{Dif}$ is diffusive penetration depth given by (Waniewski 2001):

$$\Lambda_{Dif} = \sqrt{D^T / \left(k^T + q_L\right)} \tag{22}$$

where $D^T$ is tissue diffusivity, $k^T$ is unidirectional clearance for transport from tissue to blood, and $q_L$ is tissue lymphatic absorption. The penetration depth for solutes with different molecular weight is presented in Tables 3 and 4.

*Remark* 1. In the case of purely diffusive transport across the capillary wall and the tissue, and neglected lymphatic absorption from the tissue, one can get a simplified formula $\Lambda_{Dif} = \sqrt{D^T / p_S a}$ (Dedrick et al. 1982), which shows that purely diffusive penetration depth for solutes depends on the square root of their diffusivity in the tissue divided by their diffusivity across capillary wall.

*Remark* 2. The diffusive solute penetration depth depends not only on the diffusive properties of both transport barriers. The additional correction for the lymphatic absorption from the tissue, $q_L$, fluid transport across the capillary wall, $q_V{}^{cap}$, and sieving properties of the capillary wall, $s^{cap}$, should be additionally taken into account resulting in further decrease of the solute penetration depth.

*Remark* 3. Formula (19) can be transformed to $memKBD_S = A\left(k^T + q_L\right)\cdot\Lambda_1$, which means that the effective diffusive mass transport parameter for solute transport may be considered, according to the distributed model, as proceeding directly between blood and dialysis fluid across the total capillary wall surface within the tissue layer of the width $\Lambda_1 = \Lambda_{Dif}\tanh\left(L/\Lambda_{Dif}\right)$ (where $L$ is tissue width) with the transport parameter equal to $k^T + q_L$, and these capillaries can be considered as immersed directly in dialysis fluid (Waniewski 2002; Waniewski, Werynski, and Lindholm 1999). For small solutes, $k^T + q_L$ is approximately equal to $p_S a$ (Waniewski, Werynski, and Lindholm 1999).

*Remark* 4. Formula (19) can be alternatively transformed to $memKBD_S = A\cdot D^T/\Lambda_2$ indicating that the same solute transport may be considered also as proceeding between blood and dialysis fluid across the tissue layer with solute tissue diffusivity $D^T$ and width $\Lambda_2 = \Lambda_{Dif}/\tanh\left(L/\Lambda_{Dif}\right)$ without any interference from blood flow in the capillaries (Waniewski 2002; Waniewski, Werynski, and Lindholm 1999).

*Remark* 5. Note, that for $L >> \Lambda_{Dif}$, $\Lambda_1 \approx \Lambda_2 \approx \Lambda_{Dif}$.

### 4.1.3 Effective peritoneal blood flow

In the context of peritoneal dialysis it is usually assumed that only a relatively thin layer of the tissue that is adjacent to the peritoneal surface participates effectively in the exchange of solutes between dialysate and blood. The rate of blood flow in this layer is called the effective peritoneal blood flow (EPBF). Some investigators attempted to evaluate EPBF using quickly diffusing gases, others considered the gas clearances as an overestimation of EPBF and pointed out the possibility of much lower values for EPBF as well as different EPBF values for solutes of different transport characteristics (Nolph and Twardowski 1989).

The effective peritoneal blood flow, EPBF, can be defined according to the distributed model as the blood flow in a tissue layer of the depth equal to the solute penetration depth, that is (Waniewski, Werynski, and Lindholm 1999):

$$EPBF = A\cdot q_B\cdot\Lambda_{Dif} \tag{23}$$

where $A$ is effective peritoneal surface area, $q_B$ is perfusion rate (in ml/min/g), and $\Lambda_{Dif}$ is solute diffusive penetration depth. An alternative approach to the definition of EPBF can be found in (Waniewski, Werynski, and Lindholm 1999; Waniewski 2002).

### 4.2 Combined diffusive and convective solute transport

In this section the relationships between the net diffusive mass transport coefficients for the solute transport between blood and dialysis fluid and the local physiology based transport parameters of distributed models are analyzed for combine diffusive and convective solute

transport. Inclusion of convective solute transport across the tissue is especially important in the case of macromolecules. In this section, the impact of the convective flow on the solute penetration depth as well on the effective reflection coefficient of peritoneal transport system is analyzed.

*Remark* 1. The effective peritoneal blood flow is different for different solutes, see Table 4.

| Solute | $\Lambda_{Dif}$, mm | $memKBD_S$, ml/min | $EPBF$, ml/min |
|---|---|---|---|
| $H_2$ | 0.68 | 269.6 | 269.6 |
| $CO_2$ | 0.39 | 154.6 | 154.6 |
| Urea | 0.18 | 19.8 | 52.7 |
| Creatinine | 0.18 | 14.7 | 53.8 |
| Glucose | 0.19 | 11.6 | 55.1 |
| Sucrose | 0.19 | 7.9 | 57.7 |
| Vitamin $B_{12}$ | 0.21 | 4.1 | 63.4 |
| Inulin | 0.24 | 1.9 | 71.2 |

Table 4. Theoretical values of solute penetration depth, diffusive mass transport coefficient, and perfusion rate calculated according to the distributed model assuming perfusion rate $q_B = 0.3$ ml/min/g (Waniewski, Werynski, and Lindholm 1999).

In the commonly applied phenomenological membrane models, the solute flow from dialysate to blood is typically evaluated using the following equation (Waniewski 2006, 2001):

$$J_S = KBD_S(C_D - C_B) + SJ_V[(1-F)C_D + FC_B], \tag{24}$$

where $KBD_S$ is membrane diffusive mass transport coefficient, $S$ is membrane sieving coefficient, $j_V$ is fluid flow between blood and dialysate, $C_B$ and $C_D$ are solute concentrations in blood and dialysate, respectively, and $F$ is a weighing factor for the mean concentration (Waniewski 2001). In order to compare both approaches, one may derive fro distributed model the following expression for solute flow from the peritoneal cavity to the tissue at the steady state (Waniewski 2001):

$$J_S^{perit} = memKBD_S\left(C_D - \kappa C_B\right) + s^T J_V\left(\left(1-f\right)C_D + f\kappa C_B\right). \tag{25}$$

where $memKBD_S = \sqrt{D^T(k^T + q_L)}$ is the effective diffusive transport parameter (see previous section), $\kappa = k^{cap} / \left(k^T + q_L\right)$ describes the ratio of the equilibrium concentration of solute in the tissue over its concentration in blood (see previous section), $f = 0.5 - \alpha$, $\alpha = \sqrt{1 + Pe^2/4} - 1/Pe$, and $Pe = s^T J_V / memKBD_S$ (Waniewski 2001).

### 4.2.1 Effective sieving coefficient for macromolecules

The important difference between phenomenological versus distributed approach (equations (24) and (25)) is the presence of coefficient $\kappa$ in equation (25). As it was

discussed in previous section, this parameter is typically close to 1 for small and middle molecules, whereas its values remain substantially lower than 1 for macromolecules (c.f. Table 3). In consequence, the concentration of macromolecules in dialysate equilibrates with their concentration in the tissue equal to $\kappa C_B$, instead of that in blood.

Equation (25) indicates relationship between effective sieving coefficient for macromolecules and fluid flow direction, which is not present in the membrane model. In general, the sieving coefficient may be measured directly if convective transport is prevailing, i.e. with very high fluid flow, or in isochratic conditions, i.e. during diffusive equilibrium at both sides of the membrane. If the measurement is done using solute concentration in blood as the reference, then the obtained value depends on the direction of fluid flow.

*Remark* 1. For $j_V{}^{perit} > 0$ (i.e. in the direction from peritoneal cavity to the tissue) and $Pe >> 1$ (i.e. with convective transport prevailing over diffusive one), then the measured value of sieving coefficient is equal to the sieving coefficient of solute in the tissue, $s^T$, whereas for fluid flux across the tissue in the opposite direction (i.e. $j_V{}^{perit} < 0$) and $Pe << -1$ this value is equal to $\kappa C$.

### 4.2.2 Diffusive vs. convective penetration depth

Let us consider the combine diffusive and convective solute transport at the steady state. It can be shown that the solute penetration depth can be calculated in this case as (Waniewski 2001):

$$\Lambda = \frac{{\Lambda_{Dif}}^2}{\sqrt{{\Lambda_{Dif}}^2 + {\Lambda_{Conv}}^2 / 4} - \Lambda_{Dif} / 2} \tag{26}$$

where $\Lambda_{Dif}$ is diffusive penetration depth, equation (22). The convective penetration depth for purely convective solute transport across the tissue, $\Lambda_{Conv}$, is defined as:

$$\Lambda_{Conv} = s^T j_V / \left( k^T + q_L \right) \tag{27}$$

The comparison between the overall penetration depth $\Lambda$, and its diffusive and convective components, $\Lambda_{Dif}$ and $\Lambda_{Conv}$, calculated for $J_V{}^{perit} = 1\,\text{ml/min}$ is presented in Table 5. $J_V{}^{perit} = 1\,\text{ml/min}$ is a typical value for the rate of fluid absorption from the peritoneal cavity.

*Remark* 1. For small molecules with prevailing diffusive transport (i.e. $\left|\Lambda_{Conv} / \Lambda_{Dif}\right| << 1$) the overall solute formula for the penetration depth can be simplified to $\Lambda \approx \Lambda_{Dif} + \Lambda_{Conv} / 2$ (Waniewski 2001).

*Remark* 2. In the case of solutes that are transported mainly by convection $\Lambda \approx \Lambda_{Conv}$ (for $\Lambda_{Conv} / \Lambda_{Dif} >> 1$) or, if they cannot penetrate the tissue, $\Lambda \approx 0$ (for $\Lambda_{Conv} / \Lambda_{Dif} << -1$).

*Remark* 3. That penetration depth for small solutes (creatinine) is dominated by the process of diffusion, for middle molecules (inulin, $\beta_2$-microglobulin) both processes contribute to the depth of solute penetration, and for macromolecules (albumin, IgM) the convective transport prevails, see Table 5.

| Solute | $\Lambda_{Dif}$ , mm | $\Lambda_{Conv}$ , mm | $\Lambda$ , mm |
|---|---|---|---|
| Creatinine | 0.25 | 0.03 | 0.26 |
| Inulin | 0.29 | 0.19 | 0.40 |
| $\beta_2$-microglobulin | 0.60 | 0.85 | 1.15 |
| Albumin | 0.71 | 2.63 | 2.81 |
| IgM | 0.44 | 3.40 | 3.46 |

Table 5. Penetration depth for different transport processes and for different solutes for $J_V^{perit} = 1\,\mathrm{ml/min}$ (Waniewski 2001).

## 5. Kinetics of peritoneal dialysis

The phenomenological models of the peritoneal transport such as the three-pore model or the membrane model, describe the kinetic of solute and fluid in the peritoneal cavity (Stachowska-Pietka 2010; Waniewski 2006). Complementary to them, the distributed approach allows for modeling the changes in the tissue, such as space distribution of interstitial hydrostatic pressure, tissue hydration and solute concentration in the tissue (Flessner, Dedrick, and Schultz 1985; Stachowska-Pietka et al. 2006; Waniewski, Stachowska-Pietka, and Flessner 2009; Flessner 2001). However, due to the complexity of the peritoneal phenomena as well as its high nonlinearity, distributed models are solved numerically for most applications. For example, numerical simulations of a peritoneal distributed model can be performed for a single exchange with hypertonic glucose solution 3.86%, see Figure 5 (Stachowska-Pietka and Waniewski 2011). The infusion of hypertonic solution induces water inflow into adjacent tissue. In consequence, increase of interstitial hydrostatic pressure and tissue hydration (as assessed by fluid void volume) can be observed in the tissue layer close to the peritoneal cavity (about 2.5 mm from the peritoneal surface, Figure 5, left panel) during next minutes and hours whereas the hydration of deeper tissue layers remains unchanged. Glucose diffuses from the peritoneal cavity into the tissue causing increase of glucose concentration in a thin layer of the tissue close to the peritoneal cavity (less than 0.01 cm width), c.f. Figure 5, right panel.

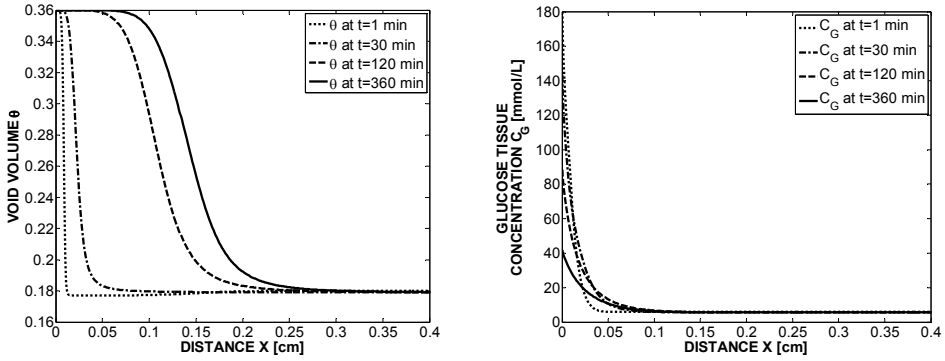


Fig. 5. Interstitial fluid void volume ratio, $\theta$ (left panel), and glucose concentration in interstitial fluid, $C_G$ (right panel) at t=1, 60, 120, and 360 min. as a function of distance from the peritoneal cavity, X (Stachowska-Pietka and Waniewski 2011).

Concomitantly to the changes in the tissue hydration and solute concentration, the intraperitoneal fluid volume and glucose concentration change with dwell time, Figure 6 (Stachowska-Pietka and Waniewski 2011). The fluid absorption from the peritoneal cavity and ultrafiltration to the cavity results in the changes of intraperitoneal volume, as observed in clinical studies (Figure 6, left panel). Moreover, due to glucose diffusion into adjacent tissue, its intraperitoneal concentration decreases during the dwell time (Figure 6, right panel). Other results on the kinetics of dialysis according to distributed approach can be found elsewhere (Seames, Moncrief, and Popovich 1990; Flessner, Dedrick, and Schultz 1985, 1984; Flessner 2001; Stachowska-Pietka 2010; Stachowska-Pietka et al. 2005; Stachowska-Pietka, Waniewski, and Lindholm 2010, 2010).

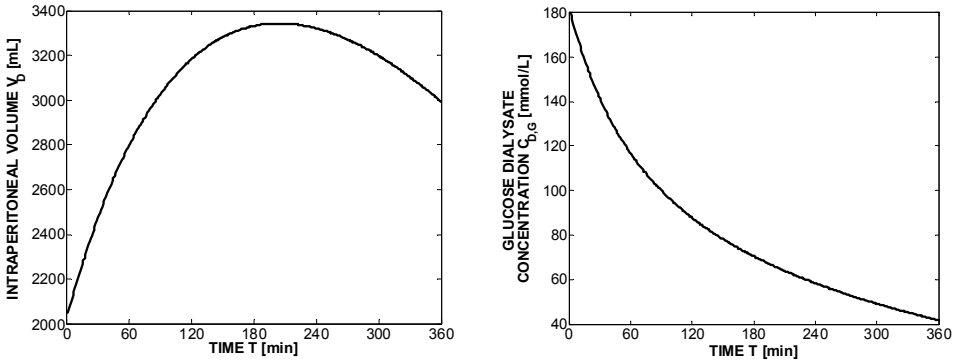


Fig. 6. Intraperitoneal volume, $V_D$, (left panel), and glucose concentration in dialysis fluid, $C_D$, (right panel) as function of dwell time T (Stachowska-Pietka and Waniewski 2011).

## 6. Conclusions

Distributed modeling allows for a detailed description of the peritoneal transport system with its real geometry and different characteristics for the main transport barriers of the capillary wall and the tissue (for most solutes of interest: the interstitium). Lymphatic absorption from the tissue, so important for the protein turnover, can also be taken into account. The models are based on the macroscopic approach with continuous distribution of the capillary and lymphatic vessels in the tissue instead of the real discrete system of these vessels. However, they can adequately describe the available data about solute concentrations and hydrostatic pressure inside the tissue during experimental studies on peritoneal dialysis (Stachowska-Pietka et al. 2006; Waniewski, Stachowska-Pietka, and Flessner 2009; Flessner 2001).

The distributed approach yields important relationships between the measurable transport parameters that are defined by the membrane models, as the diffusive mass transport parameter, hydraulic conductivity, sieving coefficient, etc., for the description of the net transport between blood and dialysis fluid in the peritoneal cavity, and the fundamental parameters for the description of the transport across the capillary wall, the tissue and lymphatic absorption from the tissue, see Figure 7. These basic local transport parameters are subject to interpatient variability and they can change with time on dialysis that may

result in serious complications in the treatment. Unfortunately, these local transport characteristics cannot be directly measured in clinical setting and one has to derive their values using mathematical models and the information from animal studies. Some of the basic questions about peritoneal transport, as the width of the tissue layer involved in the exchange of fluid and solutes during peritoneal dialysis and rate of the blood flow that participates in this exchange can be correctly answered only if the local transport coefficients are known. The formulas for the effective transport parameters, penetration depth, effective blood flow, etc., are derived from the model for the steady state transport assuming spatial homogeneity of the transport system, and therefore their application for the real dialysis may be limited for some solutes and dialysis conditions.

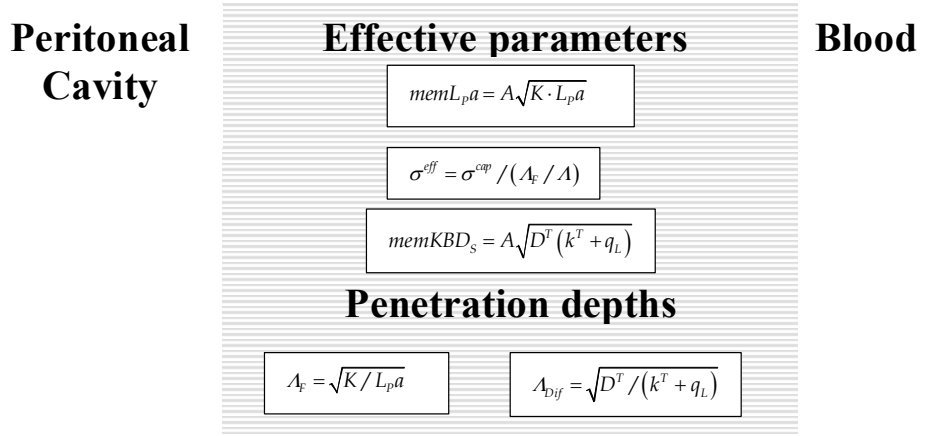


Fig. 7. Simple relationships between the effective peritoneal transport parameters and penetration depths and the local tissue and capillary wall transport parameters: $memL_Pa$ - effective hydraulic conductivity, $A$ – effective peritoneal surface area, $K$ – tissue hydraulic conductivity, $L_pa$ - capillary wall hydraulic conductance, $\sigma^{eff}$ - effective reflection coefficient, $\sigma^{cap}$ - capillary wall reflection coefficient. $\Lambda_F$ - fluid penetration depth, $\Lambda$ - solute penetration depth, $memKBD_S$ - effective diffusive transport parameters, $D^T$ - solute diffusivity in the tissue, $k^T$ - a unidirectional clearance for transport from tissue to blood, $q_L$ - tissue lymphatic absorption.

Any realistic description of peritoneal dialysis must take into account that the conditions in the peritoneal cavity and in the tissue continuously change with dwell time due to, for example, vasodilatation induced by hyperosmolality of dialysis fluid and overhydration of the tissue induced by increased hydrostatic pressure in the peritoneal cavity. Therefore, computer modeling is necessary for such a theory as shown in Section 5, see also (Stachowska-Pietka 2010).

The distributed modeling can be applied for many problems of clinical and experimental interest, and further extensions are possible. For example, the contribution of a cellular compartment in the tissue to the transport of small ions (sodium, potassium) should be taken into account (Coester et al. 2007), and a more detailed structure of the interstitium

need to be proposed to solve the problems with bidirectional transport of macromolecules (Stachowska-Pietka 2010). Nevertheless, the current understanding and quantification of the peritoneal transport obtained using the distributed approach is already a helpful tool in clinical and experimental research.

## 7. Acknowledgment

J. Stachowska-Pietka was supported by a grant N N518 417736 from the Polish Ministry of Science and Higher Education.

## 8. Nomenclature

| Symbols | Parameter |
|---|---|
| $A$ | effective peritoneal surface area, $cm^2$ |
| $C$ or $C_S$ | solute concentration in the tissue, mmol/l |
| $C_B$ or $C_{B,S}$ | solute concentration in blood, mmol/l |
| $C_D$ or $C_{D,S}$ | solute concentration in dialysate, mmol/l |
| $D^T$ or $D_S{}^T$ | solute diffusivity in the tissue, $cm^2$/min |
| $K$ | tissue hydraulic conductivity, $cm^2$/min/mmHg |
| $k^T$ | unidirectional clearance for transport from tissue to blood, 1/min |
| $L$ | tissue width, cm |
| $L_P a$ | hydraulic conductance of the capillary wall, 1/min/mmHg |
| $memKBD_S$ | effective diffusive mass transport coefficient of the PTS, mL/min |
| $memL_P a$ | effective hydraulic conductivity of the PTS, mL/min/mmHg |
| $memOsmCond$ | effective osmotic conductance of PTS, (ml/min)/(mmol/l) |
| $P$ | interstitial hydrostatic pressure, mmHg |
| $P_B$ | blood hydrostatic pressure, mmHg |
| $P_D$ | intraperitoneal hydrostatic pressure, mmHg |
| $p_S a$ | diffusive permeability of solute across the capillary wall, 1/min |
| $q_L$ | tissue lymphatic absorption, 1/min |
| $s^{cap}$ or $s_S{}^{cap}$ | sieving coefficient for solute across the capillary wall |
| $s^T$ or $s_S{}^T$ | sieving coefficient of solute in the tissue |
| $\theta$ | interstitial fluid void volume |
| $\theta_S$ | solute void volume |
| $\kappa$ | ratio of the equilibrium concentration of solute in the tissue over its concentration in blood |
| $\Lambda$ | solute overall penetration depth, cm |
| $\Lambda_{Conv}$ | solute convective penetration depth, cm |
| $\Lambda_{Dif}$ | solute diffusive penetration depth, cm |
| $\Lambda_F$ | fluid penetration depth, cm |
| $\sigma^{cap}$ or $\sigma_S{}^{cap}$ | capillary wall reflection coefficient for solute S |

| | |
|---|---|
| $\sigma^{eff}$ | effective reflection coefficient for PTS |
| $\sigma^T$ or $\sigma_S{}^T$ | tissue reflection coefficient for solute S |

## 9. References


An, K. N., and E. P. Salathe. 1976. A theory of interstitial fluid motion and its implications for capillary exchange. *Microvasc Res* 12 (2):103-19.

Baxter, L. T., and R. K. Jain. 1989. Transport of fluid and macromolecules in tumors. I. Role of interstitial pressure and convection. *Microvasc Res* 37 (1):77-104.

———. 1990. Transport of fluid and macromolecules in tumors. II. Role of heterogeneous perfusion and lymphatics. *Microvasc Res* 40 (2):246-63.

———. 1991. Transport of fluid and macromolecules in tumors. III. Role of binding and metabolism. *Microvasc Res* 41 (1):5-23.

Cherniha, R., and J. Waniewski. 2005. Exact solutions of a mathematical model fro fluid transport in peritoneal dialysis. *Ukrainian Math. Journal* 57 (8):1112-1119.

Coester, A. M., D. G. Struijk, W. Smit, D. R. de Waart, and R. T. Krediet. 2007. The cellular contribution to effluent potassium and its relation to free water transport during peritoneal dialysis. *Nephrol Dial Transplant* 22 (12):3593-600.

Collins, J. M. 1981. Inert gas exchange of subcutaneous and intraperitoneal gas pockets in piglets. *Respir Physiol* 46 (3):391-404.

Collins, J. M., R. L. Dedrick, M. F. Flessner, and A. M. Guarino. 1982. Concentration-dependent disappearance of fluorouracil from peritoneal fluid in the rat: experimental observations and distributed modeling. *J Pharm Sci* 71 (7):735-8.

Dedrick, R. L., M. F. Flessner, J. M. Collins, and J. S. Schultz. 1982. Is the peritoneum a membrane? *ASAIO J* 5:1-8.

Flessner, M. F. 1994. Osmotic barrier of the parietal peritoneum. *Am J Physiol* 267 (5 Pt 2):F861-70.

———. 2001. Transport of protein in the abdominal wall during intraperitoneal therapy. I. Theoretical approach. *Am J Physiol Gastrointest Liver Physiol* 281 (2):G424-37.

———. 2005. The transport barrier in intraperitoneal therapy. *Am J Physiol Renal Physiol* 288 (3):F433-42.

———. 2009. Intraperitoneal Chemotherapy. In *Nolph and Gokal's textbook of peritoneal dialysis*, edited by R. Khanna and R. T. Krediet. USA: Springer.

Flessner, M. F., J. Choi, H. Vanpelt, Z. He, K. Credit, J. Henegar, and M. Hughson. 2006. Correlating structure with solute and water transport in a chronic model of peritoneal inflammation. *Am J Physiol Renal Physiol* 290 (1):F232-40.

Flessner, M. F., R. L. Dedrick, and J. S. Schultz. 1984. A distributed model of peritoneal-plasma transport: theoretical considerations. *Am J Physiol* 246 (4 Pt 2):R597-607.

———. 1985. A distributed model of peritoneal-plasma transport: analysis of experimental data in the rat. *Am J Physiol* 248 (3 Pt 2):F413-24.

———. 1985. Exchange of macromolecules between peritoneal cavity and plasma. *Am J Physiol* 248 (1 Pt 2):H15-25.

Flessner, M. F., J. D. Fenstermacher, R. L. Dedrick, and R. G. Blasberg. 1985. A distributed model of peritoneal-plasma transport: tissue concentration gradients. *Am J Physiol* 248 (3 Pt 2):F425-35.

Flessner, M. F., J. Lofthouse, and R. Zakaria el. 1997. In vivo diffusion of immunoglobulin G in muscle: effects of binding, solute exclusion, and lymphatic removal. *Am J Physiol* 273 (6 Pt 2):H2783-93.

Flessner, M., J. Henegar, S. Bigler, and L. Genous. 2003. Is the peritoneum a significant transport barrier in peritoneal dialysis? *Perit Dial Int* 23 (6):542-9.

Gupta, E., M. G. Wientjes, and J. L. Au. 1995. Penetration kinetics of 2',3'-dideoxyinosine in dermis is described by the distributed model. *Pharm Res* 12 (1):108-12.

Imholz, A. L., G. C. Koomen, D. G. Struijk, L. Arisz, and R. T. Krediet. 1993. Effect of dialysate osmolarity on the transport of low-molecular weight solutes and proteins during CAPD. *Kidney Int* 43 (6):1339-46.

Kagan, A., Y. Bar-Khayim, Z. Schafer, and M. Fainaru. 1990. Kinetics of peritoneal protein loss during CAPD: I. Different characteristics for low and high molecular weight proteins. *Kidney Int* 37 (3):971-9.

Leypoldt, J. K. 1993. Interpreting peritoneal membrane osmotic reflection coefficients using a distributed model of peritoneal transport. *Adv Perit Dial* 9:3-7.

Leypoldt, J. K., and L. W. Henderson. 1992. The effect of convection on bidirectional peritoneal solute transport: predictions from a distributed model. *Ann Biomed Eng* 20 (4):463-80.

Nolph, K. D., F. Miller, J. Rubin, and R. Popovich. 1980. New directions in peritoneal dialysis concepts and applications. *Kidney Int Suppl* 10:S111-6.

Nolph, K. D., and Z. J. Twardowski. 1989. The peritoneal dialysis system. In *Peritoneal Dialysis*, edited by K. D. Nolph. Dordrecht: Kluwer.

Pannekeet, M. M., A. L. Imholz, D. G. Struijk, G. C. Koomen, M. J. Langedijk, N. Schouten, R. de Waart, J. Hiralall, and R. T. Krediet. 1995. The standard peritoneal permeability analysis: a tool for the assessment of peritoneal permeability characteristics in CAPD patients. *Kidney Int* 48 (3):866-75.

Patlak, C. S., and J. D. Fenstermacher. 1975. Measurements of dog blood-brain transfer constants by ventriculocisternal perfusion. *Am J Physiol* 229 (4):877-84.

Perl, W. 1962. Heat and matter distribution in body tissues and the determination of tissue blood flow by local clearance methods. *J Theor Biol* 2:201-235.

———. 1963. An extension of the diffusion equation to include clearance by capillary blood flow. *Ann N Y Acad Sci* 108:92-105.

Piiper, J., R. E. Canfield, and H. Rahn. 1962. Absorption of various inert gases from subcutaneous gas pockets in rats. *J Appl Physiol* 17:268-74.

Rippe, B., and G. Stelin. 1989. Simulations of peritoneal solute transport during CAPD. Application of two-pore formalism. *Kidney Int* 35 (5):1234-44.

Rubin, J., T. Adair, Q. Jones, and E. Klein. 1985. Inhibition of peritoneal protein losses during peritoneal dialysis in dogs. *ASAIO J* 8:234-237.

Seames, E. L., J. W. Moncrief, and R. P. Popovich. 1990. A distributed model of fluid and mass transfer in peritoneal dialysis. *Am J Physiol* 258 (4 Pt 2):R958-72.

Stachowska-Pietka, J. 2010. Mathematical modeling of ultrafiltration and fluid absorption during peritoneal dialysis. PhD Thesis, Institute of Biocybernetics and Biomedical Engineering Polish Academy of Sciences, Warsaw.

Stachowska-Pietka, J., and J. Waniewski. 2011. Distributed modeling of glucose induced osmotic fluid flow during single exchange with hypertonic glucose solution. *Biocybernetics and Biomedical Engineering* 31 (1):39-50.

Stachowska-Pietka, J., J. Waniewski, M. F. Flessner, and B. Lindholm. 2006. Distributed model of peritoneal fluid absorption. *Am J Physiol Heart Circ Physiol* 291 (4):H1862-74.

———. 2007. A distributed model of bidirectional protein transport during peritoneal fluid absorption. *Adv Perit Dial* 23:23-7.

Stachowska-Pietka, J., J. Waniewski, M. Flessner, and B. Lindholm. 2005. A mathematical model of peritoneal fluid absorption in the tissue. *Adv Perit Dial* 21:9-12.

Stachowska-Pietka, J., J. Waniewski, and B. Lindholm. 2010. Bidirectional transport of fluid and protein during peritoneal dialysis assessed by distributed model with structured interstitium. *Perit Dial Int* 30 (Suppl. 2):S44.

———. 2010. Integrated distributed model of fluid and solute transport during peritoneal dialysis. *Perit Dial Int* 30 (Suppl. 1):S20.

Taylor, D. G., J. L. Bert, and B. D. Bowen. 1990. A mathematical model of interstitial transport. I. Theory. *Microvasc Res* 39 (3):253-78.

Van Liew, H. D. 1968. Coupling of diffusion and perfusion in gas exit from subcutaneous pocket in rats. *Am J Physiol* 214 (5):1176-85.

Venturoli, D., and B. Rippe. 2001. Transport asymmetry in peritoneal dialysis: application of a serial heteroporous peritoneal membrane model. *Am J Physiol Renal Physiol* 280 (4):F599-606.

Waniewski, J. 2001. Physiological interpretation of solute transport parameters for peritoneal dialysis. *J Theor Med* 3:177-190.

———. 2002. Distributed modeling of diffusive solute transport in peritoneal dialysis. *Ann Biomed Eng* 30 (9):1181-95.

———. 2006. Mathematical modeling of fluid and solute transport in hemodialysis and peritoneal dialysis. *J Mem Sci* 274:24-37.

Waniewski, J., V. Dutka, J. Stachowska-Pietka, and R. Cherniha. 2007. Distributed modeling of glucose-induced osmotic flow. *Adv Perit Dial* 23:2-6.

Waniewski, J., J. Stachowska-Pietka, and M. F. Flessner. 2009. Distributed modeling of osmotically driven fluid transport in peritoneal dialysis: theoretical and computational investigations. *Am J Physiol Heart Circ Physiol* 296 (6):H1960-8.

Waniewski, J., A. Werynski, and B. Lindholm. 1999. Effect of blood perfusion on diffusive transport in peritoneal dialysis. *Kidney Int* 56 (2):707-13.

Wientjes, M. G., R. A. Badalament, R. C. Wang, F. Hassan, and J. L. Au. 1993. Penetration of mitomycin C in human bladder. *Cancer Res* 53 (14):3314-20.

Wientjes, M. G., J. T. Dalton, R. A. Badalament, J. R. Drago, and J. L. Au. 1991. Bladder wall penetration of intravesical mitomycin C in dogs. *Cancer Res* 51 (16):4347-54.

Wiig, H., M. DeCarlo, L. Sibley, and E. M. Renkin. 1992. Interstitial exclusion of albumin in rat tissues measured by a continuous infusion method. *Am J Physiol* 263 (4 Pt 2):H1222-33.

Zakaria, E. R., J. Lofthouse, and M. F. Flessner. 1999. In vivo effects of hydrostatic pressure on interstitium of abdominal wall muscle. *Am J Physiol* 276 (2 Pt 2):H517-29.

———. 2000. Effect of intraperitoneal pressures on tissue water of the abdominal muscle. *Am J Physiol Renal Physiol* 278 (6):F875-85.

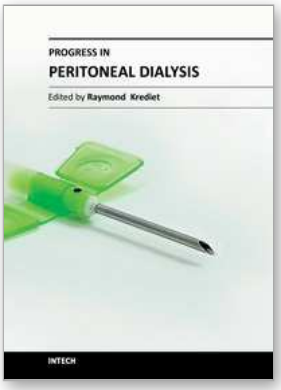


**Progress in Peritoneal Dialysis**
Edited by Dr. Ray Krediet

ISBN 978-953-307-390-3
Hard cover, 184 pages
**Publisher** InTech
**Published online** 17, October, 2011
**Published in print edition** October, 2011

Progress in Peritoneal Dialysis is based on judgement of a number of abstracts, submitted by interested people involved in various aspects of peritoneal dialysis. The book has a wide scope, ranging from in-vitro experiments, mathematical modelling, and clinical studies. The interested reader will find state of the art essays on various aspects of peritoneal dialysis relevant to expand their knowledge on this underused modality of renal replacement therapy.

**How to reference**
In order to correctly reference this scholarly work, feel free to copy and paste the following:

Joanna Stachowska-Pietka and Jacek Waniewski (2011). Distributed Models of Peritoneal Transport, Progress in Peritoneal Dialysis, Dr. Ray Krediet (Ed.), ISBN: 978-953-307-390-3, InTech, Available from: http://www.intechopen.com/books/progress-in-peritoneal-dialysis/distributed-models-of-peritoneal-transport

INTECH
open science | open minds

**InTech Europe**
University Campus STeP Ri
Slavka Krautzeka 83/A
51000 Rijeka, Croatia
Phone: +385 (51) 770 447
Fax: +385 (51) 686 166
www.intechopen.com

**InTech China**
Unit 405, Office Block, Hotel Equatorial Shanghai
No.65, Yan An Road (West), Shanghai, 200040, China
中国上海市延安西路65号上海国际贵都大饭店办公楼405单元
Phone: +86-21-62489820
Fax: +86-21-62489821